

Electronic Supplementary Information

Changes in Macrocyclic Aromaticity and Formation of Charge-separated State by Complexation of Expanded Porphyrin and C₆₀

Won-Young Cha,^{ad} Ahreum Ahn,^c Taeyeon Kim,^a Juwon Oh,^a Rashid Ali,^b Jung Su Park,^{*b} and Dongho Kim^{*a}

^aDepartment of Chemistry and Spectroscopy Laboratory for Functional π -Electronic Systems,
Yonsei University, Seoul 03722, Korea

^bDepartment of Chemistry, Sookmyung Women's University, 100 Cheongpa-ro 47-gil, Yongsan-
gu, Seoul 04310, Republic of Korea

^cCenter for Supercomputing Applications, Korea Institute of Science and Technology
Information, 245 Daehak-ro, Daejeon 34141, Republic of Korea

^dDepartment of Molecular Engineering, Graduate School of Engineering, Kyoto University,
Katsura, Nishikyo-ku, Kyoto 615-8510, Japan.

E-mail: dongho@yonsei.ac.kr (D. Kim), jspark@sookmyung.ac.kr (J. S. Park)

Experimental Details

Sample preparation and steady-state measurements

Details of the synthesis, characterization, and X-ray crystallographic analysis of **1** are described elsewhere.¹ HPLC-grade solvents were purchased from Sigma-Aldrich and used without further purification. Steady-state absorption spectra were measured on a UV/Vis/NIR spectrometer (Varian, Cary5000) and fluorescence spectra in the range of visible wavelength region were measured on a fluorescence spectrophotometer (Hitachi, F-2500). Fluorescence spectra are spectrally corrected by using correction factor of the fluorescence spectrophotometer. The NIR fluorescence was detected using a monochromator (Acton Research, SP2150) with a focal length of 15 cm attached to a near-infrared (NIR) photomultiplier (Hamamatsu, H9170-75) and a lock-in amplifier (EG&G, DSP-5210) combined with a mechanical chopper and recorded after laser excitation at 442 nm from a continuous wave (CW) He-Cd laser (Melles Griot, Omnicrome 74). A quartz cell (Hellma) with a 10 mm optical path length was used for all steady-state measurements.

Computational Methods

Quantum chemical calculations were performed with the Gaussian 16 program.² Full geometry optimizations of the host **1** and complex **1**:C₆₀ were calculated using density functional theory (DFT)³⁻⁴ Becke's three-parameter hybrid function with the non-local correlation of Lee-Yang-Parr (B3LYP)⁵ method in gas phase. We calculated all of the above calculations were using 6-31G(d)⁶⁻⁹ basis set. Also, In order to include the solvent polarization effect was used in calculation for the host **1** and complex **1**:C₆₀ in toluene. Polarized Continuum Model (PCM)¹⁰⁻¹¹ for the ground state geometry optimization. After optimization, absolute ¹H NMR chemical shifts were calculated with the GIAO¹²⁻¹⁶ method using corresponding TMS shielding calculated at the same theoretical level.

Femtosecond Transient Absorption Measurements. Femtosecond time-resolved transient absorption (*fs*-TA) spectra were recorded on a spectrometer consisting of an Optical Parametric Amplifier (OPA) (Palitra, Quantronix) pumped by a Ti:sapphire regenerative amplifier system (Integra-C, Quantronix) operating at a 1 kHz repetition rate in conjunction with an optical

detection system. The generated OPA pulses had a pulse width of ~ 100 fs and an average power of 100 mW in the range 280-2700 nm and were used as pump pulses. White light continuum (WLC) probe pulses were generated using a sapphire window (3 mm of thickness) by focusing a small number of the fundamental 800 nm pulses, which were picked off by a quartz plate before entering into the OPA. The time delay between pump and probe beams was carefully controlled by making the pump beam travel along a variable optical delay (ILS250, Newport). The intensities of the spectrally dispersed WLC probe pulses were monitored by a high speed spectrometer (Ultrafast Systems). To obtain the time-resolved transient absorption difference signal (ΔA) at a specific time, the pump pulses were chopped at 500 Hz and the absorption spectral intensities were saved alternately with or without the pump pulse. Typically, 4000 pulses were used to excite the samples and to obtain the fs-TA spectra at a particular delay time. The polarization angle between the pump and probe beams was set at the magic angle (54.7°) using a Glan-laser polarizer with a half-wave retarder in order to prevent polarization-dependent signals. The cross-correlation FWHM in the pump-probe experiments was less than 200 fs and the chirp of WLC probe pulses was measured to be 800 fs in the 400-800 nm region. To minimize chirp, all-reflection optics in the probe beam path and the 2 mm path length of quartz cell were used. After the fluorescence and fs-TA experiments, the absorption spectra of all compounds were checked to determine if there were artifacts due to sample degradation or photo-oxidation. HPLC grade solvents were used in all steady-state and time-resolved spectroscopic studies. The three-dimensional data sets of ΔA versus time and wavelength were subjected to singular value decomposition and global fitting to obtain the kinetic time constants and their associated spectra using Surface Explorer software (Ultrafast Systems).

Nanosecond Transient Absorption Measurements. Nanosecond transient absorption spectra were measured using a nanosecond flash photolysis technique. Excitation pulses are tuned by using Surelite OPO (optical parametric oscillator) pumped by 355 nm with a time duration of ca. 6 ns and energy of ca. 2 mJ/pulse were generated from the third harmonic output of a Continuum model Surelite Q-switched Nd:YAG laser. The probe light generated by a cw Xe lamp (150 W) was collimated on the sample cell and then spectrally resolved by using a Acton Research model SP150 monochromator (15 cm) equipped with a 600 grooves/mm grating with a spectral resolution of about 3 nm. The light signal was detected by using a Si avalanche

photodiode (Hamamatsu, model C5331), and recorded with a 500 MHz digital storage oscilloscope (Tektronix, model TDS3052). To ensure the data, we first examined the triplet state dynamics of zinc (II) tetraphenylporphyrin in toluene at 25 °C, which gave the lifetime of 1 ms.

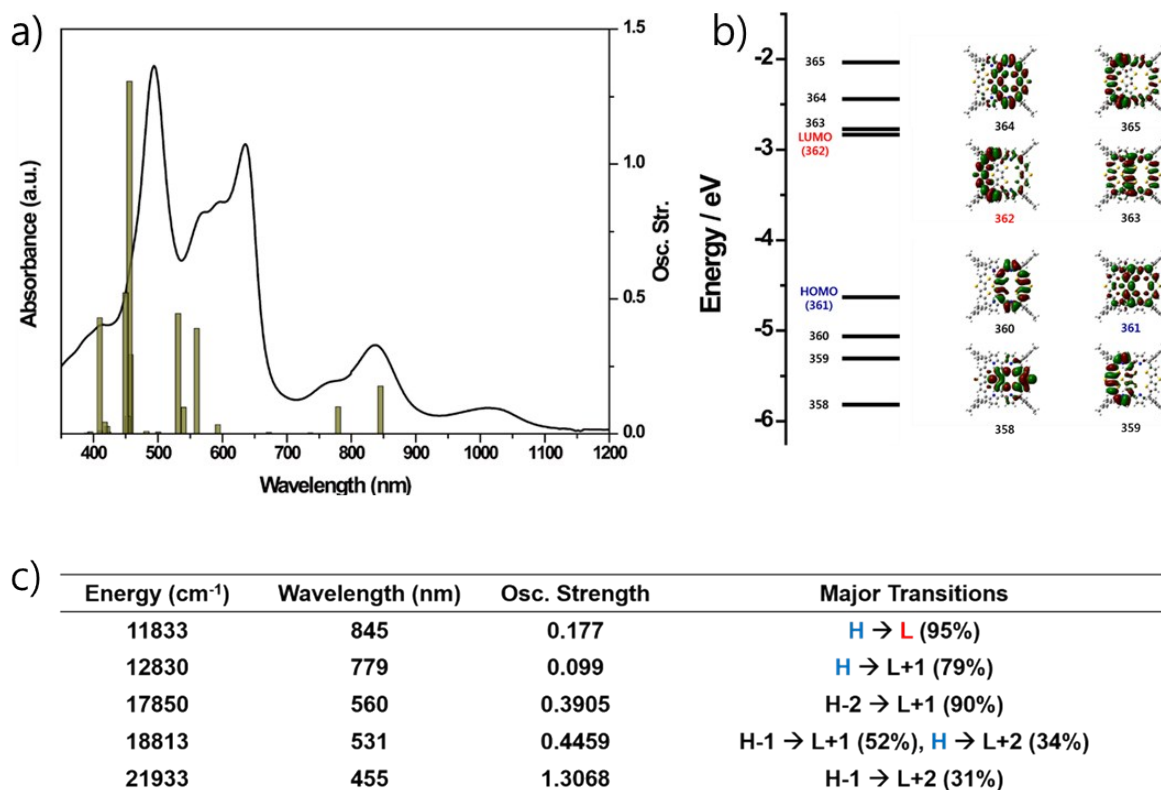


Fig. S1 a) Calculated electronic vertical transitions, b) energy levels and molecular orbitals, and c) major transitions of free host **1** calculated by TDDFT using B3LYP employing the 6-31G(d) basis set.

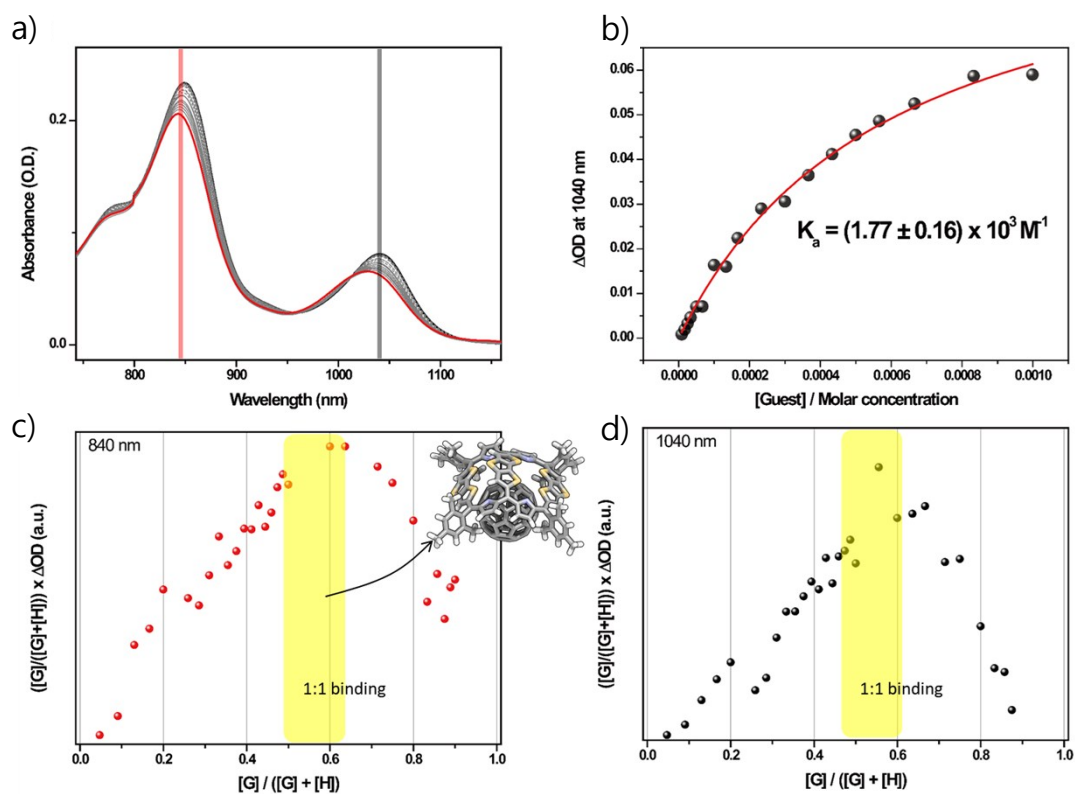


Fig. S2 a) Partial views of the absorption spectral changes upon addition of C₆₀ up to 30 equivalents. b) Nonlinear fitting of ΔA at 1040 nm to 1:1 binding profile; the inset shows the resulting association constant, K_a . Job plots constructed from absorption spectral changes both at c) 840 and d) 1040 nm demonstrating the 1:1 stoichiometry.

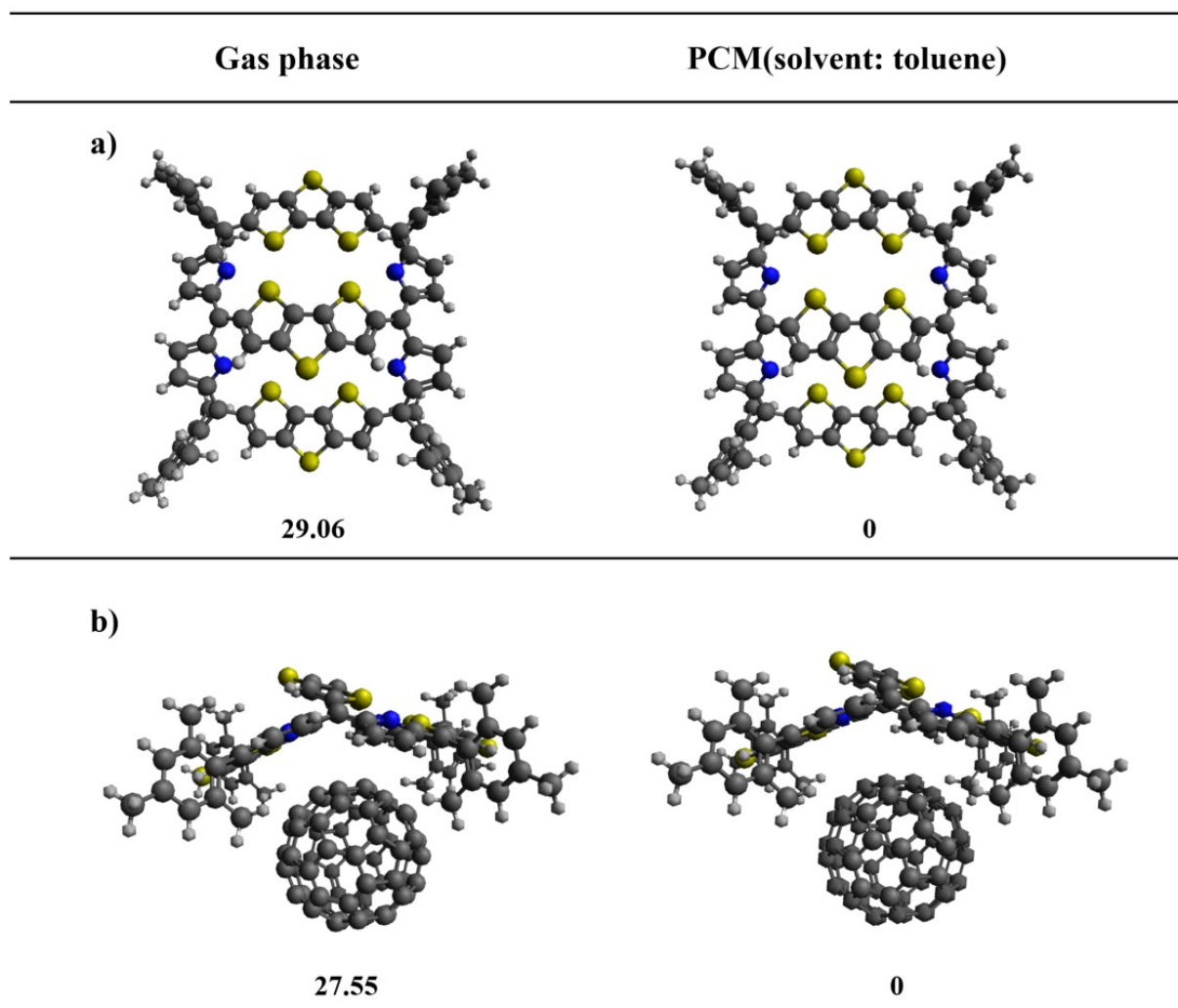


Fig. S3 Optimized structures and relative energies (in kJ/mol) of a) **1** and b) **1:C₆₀** calculated at the B3LYP with a 6-31G(d) and B3LYP with a 6-31G(d)/PCM(toluene).

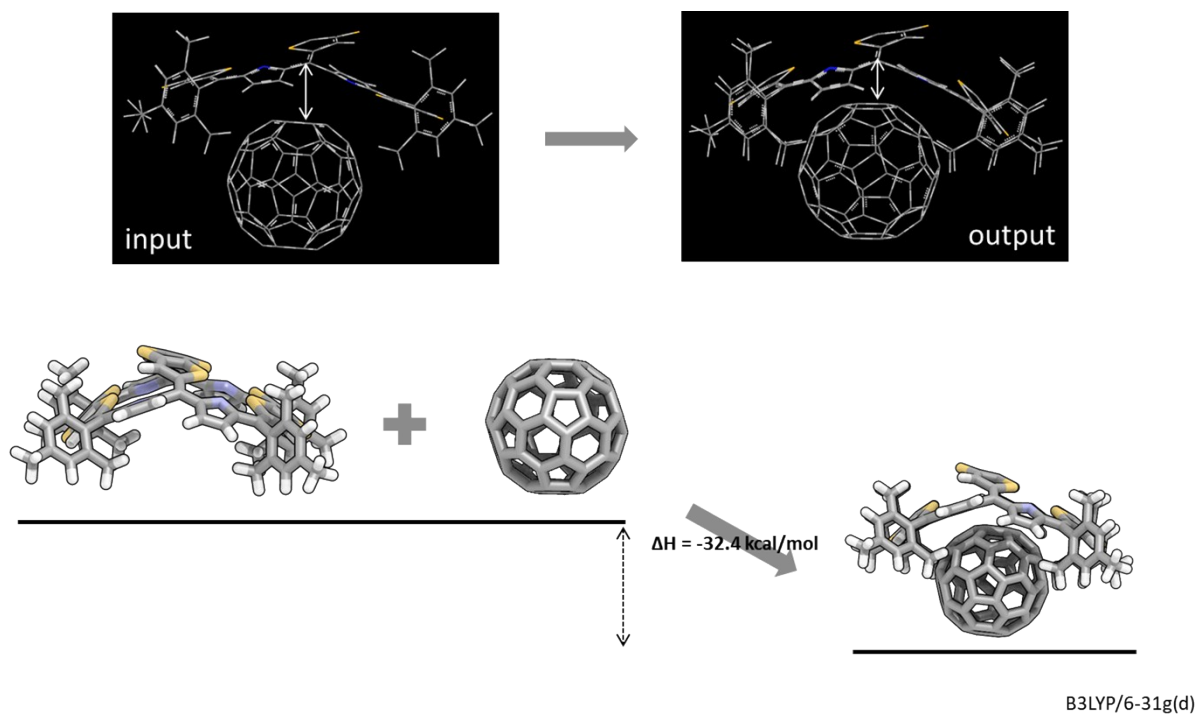


Fig. S4 Input and optimized structures of complex **1:C₆₀** and their binding energies compared to **pristine 1** and **C₆₀**.

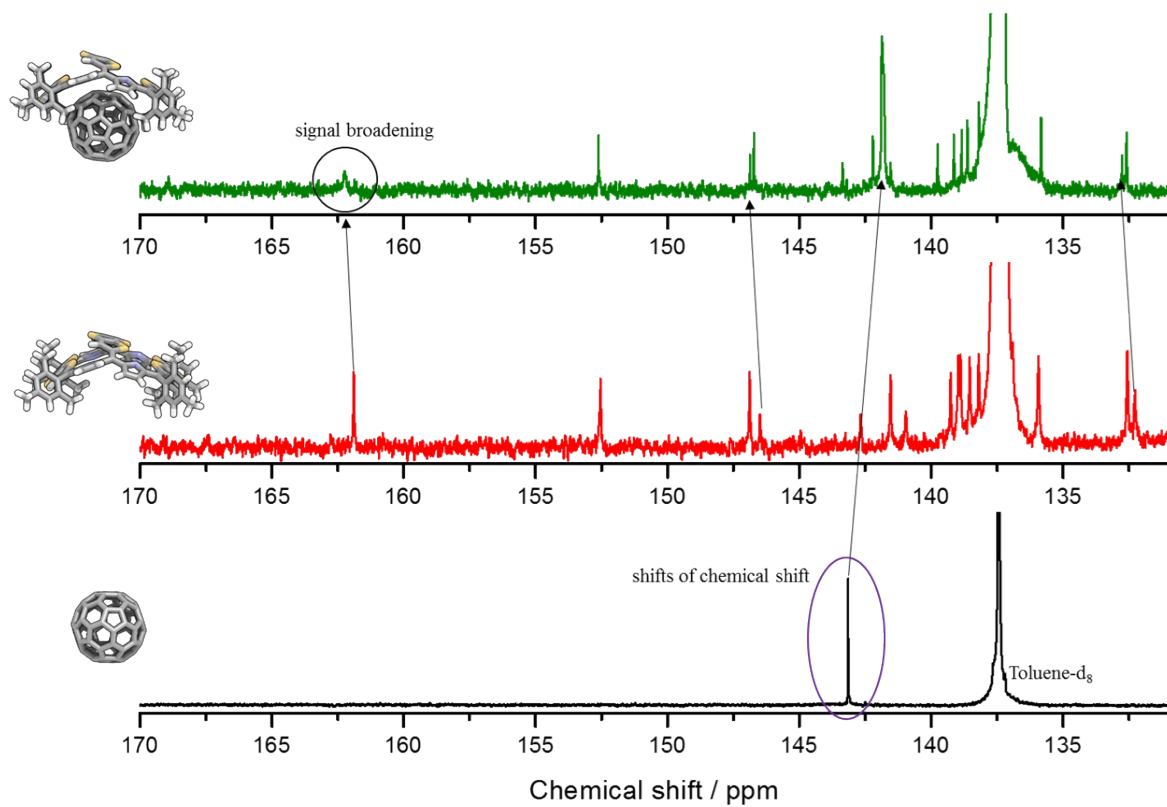


Fig. S5 Partial views of the carbon NMR spectra of complex **1**:C₆₀, free host **1**, and C₆₀ in toluene-d₈ at 293 K.

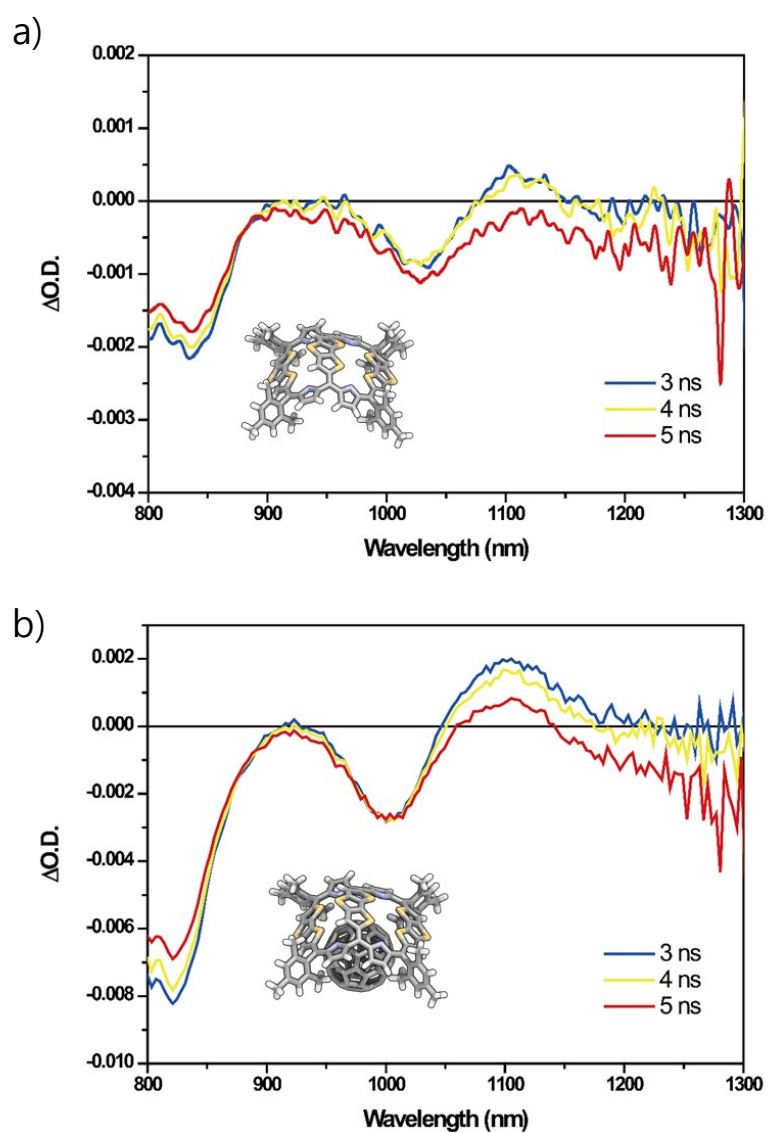


Fig. S6 *fs*-TA spectra a) **1** and b) **1:C₆₀** in the NIR region at the time delays of 3, 4, and 5 ns.

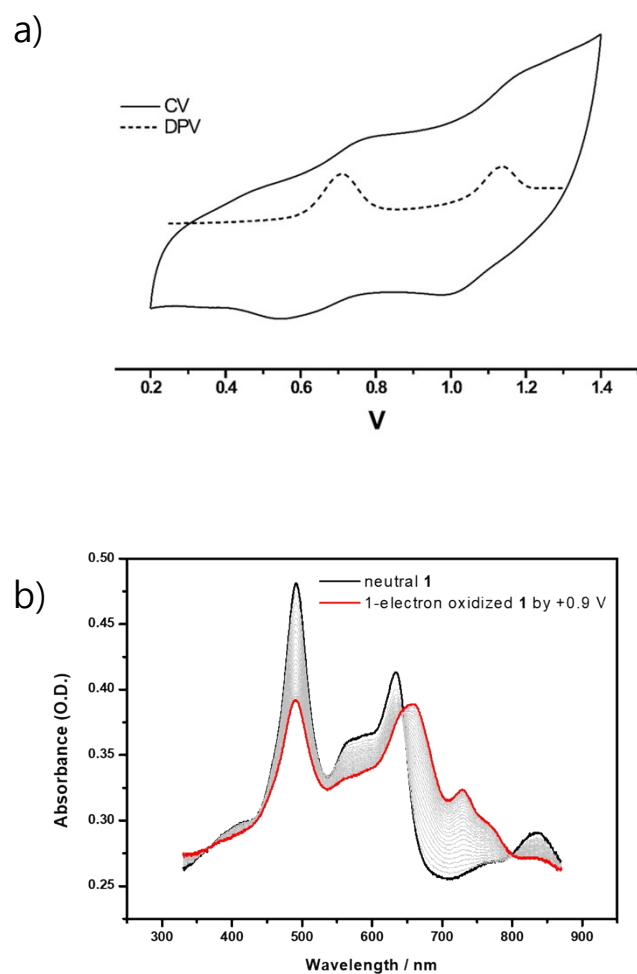


Fig. S7 a) Cyclic and differential pulse voltammograms of free host **1**. Supporting electrolyte: 0.10 M tetrabutylammonium hexafluorophosphate in $\text{CH}_2\text{Cl}_2/\text{acetonitrile}$ (4:1 ratio); working electrode: glassy carbon rod; counter electrode: platinum wire; reference electrode: $\text{Ag}/0.01\text{M}$ AgClO_4 . b) Oxidative electrochemical titrations carried out at the first oxidation potential of 0.9 V.

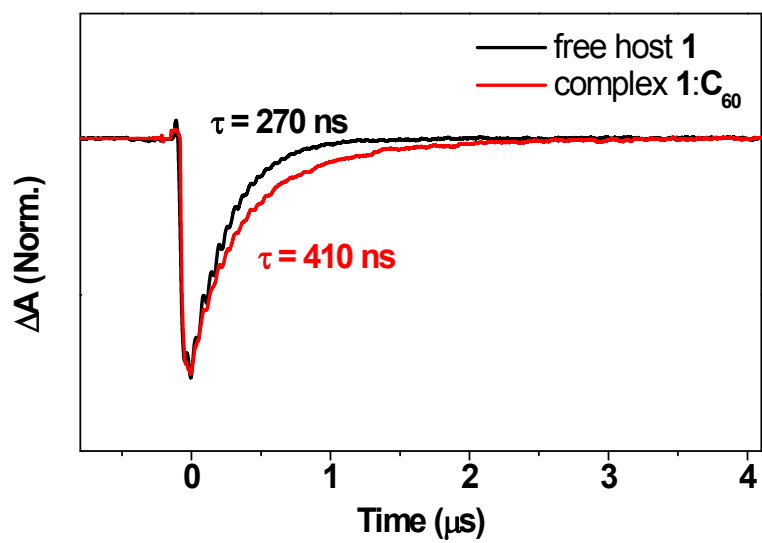


Fig. S8 Decay profiles and triplet lifetimes of a) free host **1** and b) complex **1**:C₆₀ in toluene/paraffin oil (1:19) measured by nanosecond flash photolysis technique

Notes and references

1. Cha, W.-Y.; Kim, T.; Ghosh, A.; Zhang, Z.; Ke, X.-S.; Ali, R.; Lynch, V. M.; Jung, J.; Kim, W.; Lee, S.; Fukuzumi, S.; Park, J. S.; Sessler, J. L.; Chandrashekar, T. K.; Kim, D., Bicyclic Baird-type Aromaticity. *Nature Chemistry*, **2017**, *9*, 1243–1248
2. Frisch, M. J.; Trucks, G. W.; Schlegel, H. B.; Scuseria, G. E.; Robb, M. A.; Cheeseman, J. R.; Scalmani, G.; Barone, V.; Petersson, G. A.; Nakatsuji, H.; Li, X.; Caricato, M.; Marenich, A. V.; Bloino, J.; Janesko, B. G.; Gomperts, R.; Mennucci, B.; Hratchian, H. P.; Ortiz, J. V.; Izmaylov, A. F.; Sonnenberg, J. L.; Williams; Ding, F.; Lipparini, F.; Egidi, F.; Goings, J.; Peng, B.; Petrone, A.; Henderson, T.; Ranasinghe, D.; Zakrzewski, V. G.; Gao, J.; Rega, N.; Zheng, G.; Liang, W.; Hada, M.; Ehara, M.; Toyota, K.; Fukuda, R.; Hasegawa, J.; Ishida, M.; Nakajima, T.; Honda, Y.; Kitao, O.; Nakai, H.; Vreven, T.; Throssell, K.; Montgomery Jr., J. A.; Peralta, J. E.; Ogliaro, F.; Bearpark, M. J.; Heyd, J. J.; Brothers, E. N.; Kudin, K. N.; Staroverov, V. N.; Keith, T. A.; Kobayashi, R.; Normand, J.; Raghavachari, K.; Rendell, A. P.; Burant, J. C.; Iyengar, S. S.; Tomasi, J.; Cossi, M.; Millam, J. M.; Klene, M.; Adamo, C.; Cammi, R.; Ochterski, J. W.; Martin, R. L.; Morokuma, K.; Farkas, O.; Foresman, J. B.; Fox, D. J. *Gaussian 16 Rev. B.01*, Wallingford, CT, 2016.
3. Becke, A. D., Density-functional exchange-energy approximation with correct asymptotic behavior. *Physical Review A* **1988**, *38* (6), 3098-3100.
4. Runge, E.; Gross, E. K. U., Density-Functional Theory for Time-Dependent Systems. *Physical Review Letters* **1984**, *52* (12), 997-1000.
5. D. Becke, A., *Density-Functional Thermochemistry. III. The Role of Exact Exchange*. 1993; Vol. 98, p 5648-5653.
6. Petersson, a.; Bennett, A.; Tensfeldt, T. G.; Al-Laham, M. A.; Shirley, W. A.; Mantzaris, J., A complete basis set model chemistry. I. The total energies of closed-shell atoms and hydrides of the first-row elements. *The Journal of chemical physics* **1988**, *89* (4), 2193-2218.
7. Petersson, G.; Al-Laham, M. A., A complete basis set model chemistry. II. Open-shell systems and the total energies of the first-row atoms. *The Journal of chemical physics* **1991**, *94* (9), 6081-6090.
8. Hehre, W. J.; Ditchfield, R.; Pople, J. A., Self-consistent molecular orbital methods. XII. Further extensions of gaussian-type basis sets for use in molecular orbital studies of organic molecules. *The Journal of Chemical Physics* **1972**, *56* (5), 2257-2261.
9. Ditchfield, R.; Hehre, W. J.; Pople, J. A., Self-consistent molecular-orbital methods. IX. An extended Gaussian-type basis for molecular-orbital studies of organic molecules. *The Journal of Chemical Physics* **1971**, *54* (2), 724-728.
10. Mennucci, B.; Tomasi, J.; Cammi, R.; Cheeseman, J. R.; Frisch, M. J.; Devlin, F. J.; Gabriel, S.; Stephens, P. J., Polarizable Continuum Model (PCM) Calculations of Solvent Effects on Optical Rotations of Chiral Molecules. *The Journal of Physical Chemistry A* **2002**, *106* (25), 6102-6113.
11. Tomasi, J.; Mennucci, B.; Cammi, R., Quantum Mechanical Continuum Solvation Models. *Chemical Reviews* **2005**, *105* (8), 2999-3094.
12. Cheeseman, J.; Trucks, G.; A. Keith, T.; J. Frisch, M., *A Comparison of Models for Calculating Nuclear Magnetic Resonance Shielding Tensors*. 1996; Vol. 104, p 5497-5509.
13. Ditchfield, R., Self-consistent perturbation theory of diamagnetism. *Molecular Physics* **1974**, *27* (4),

789-807.

14. London, F., Théorie quantique des courants interatomiques dans les combinaisons aromatiques. *J. Phys. Radium* **1937**, 8 (10), 397-409.
15. McWeeny, R., Perturbation Theory for the Fock-Dirac Density Matrix. *Physical Review* **1962**, 126 (3), 1028-1034.
16. Wolinski, K.; Hinton, J. F.; Pulay, P., Efficient implementation of the gauge-independent atomic orbital method for NMR chemical shift calculations. *Journal of the American Chemical Society* **1990**, 112 (23), 8251-8260.